DOI: 10.1002/ejic.201000729

Various Synthetic Methods for One-Dimensional Semiconductor Nanowires/Nanorods and Their Applications in Photovoltaic Devices

Jinyoung Chun[a] and Jinwoo Lee*[a]

Keywords: Semiconductors / Template synthesis / Synthetic methods / Nanostructures / Colloids

In this microreview, the recent progress on various synthetic methods for 1D semiconductor nanowires is summarized. The colloidal synthetic method has been popularly employed to prepare various semiconductor nanorods/nanowires such as ZnS and TiO_2. The vapor–liquid–solid (VLS) synthetic method has been used to fabricate Si and ZnO nanowires. For the growth of semiconductor nanowires by the VLS method, metals that can form a eutectic mixture with a target material have been used as catalysts. After the first report on the synthesis of crystalline III–V semiconductor nanowires by the solution–liquid–solid (SLS) method, various kinds of III–V and II–VI semiconductor nanowires have been synthesized by the SLS method. Various types of templates, including anodic aluminum oxide (AAO), sacrificial nanowire templates, and self-assembled surfactants, have been employed to fabricate 1D semiconductor nanowires that resemble the shape of the template employed. Using 1D semiconductor nanowires, high-performance photovoltaic cells can be fabricated due to facile electron transport within nanowires.

Introduction

We expect that current technology can be greatly improved with the aid of nanotechnology, which emerged in the 1990s. Nanomaterials have been extensively studied and new synthetic methods have been developed to fabricate desired nanomaterials for specific applications in various fields. It is usually accepted that interesting physical properties and new phenomena can be observed when the size of semiconductor materials is decreased to the nanometer scale.[1] The first synthesis of II–VI semiconductor nanocrystals through the colloidal synthetic method (the so-called "hot-injection" method) was reported by Murray, Norris, and Bawendi in 1993.[2] Their synthesis was based on the thermal decomposition of organometallic precursors in high-temperature organic solvent. They opened new avenues for the preparation of semiconductor nanostructured materials. This synthetic method was extended to other semiconductor nanocrystals such as ZnS,[3] CdTe,[4] InAs,[5] and CdSe/ZnS core–shell structures.[6]

Along with size-dependent physical properties of semiconductor nanomaterials, the study of shape-dependent properties of semiconductor nanomaterials is of great importance for practical application of nanomaterials. The development of semiconductor nanowires/nanorods will pro-

[a] Department of Chemical Engineering,
School of Environmental Science and Engineering,
Pohang University of Science and Technology,
san 31, Hyo-ja dong, Pohang, 790-784, Korea
E-mail: jinwoo03@postech.ac.kr

Jinyoung Chun received his B.S. degree from the Department of Chemical and Biological Engineering of Seoul National University in 2007. As a graduate student in an integrated Ph.D. course, he has studied at the Pohang University of Science and Technology (POSTECH) since 2009. He is working on the synthesis of nanostructured materials and their application in fuel cells and solar cells under the guidance of Prof. Jinwoo Lee.

Prof. Jinwoo Lee obtained his B.S. (1998), M.S. (2000), and Ph.D. (2003) from the Department of Chemical and Biological Engineering of Seoul National University, Korea. After his postdoctoral research at Seoul National University (with Prof. Taeghwan Hyeon, 2003–2005) and Cornell University (with Prof. Ulrich Wiesner, 2005–2008), he joined the faculty of the Department of Chemical Engineering at Pohang University of Science and Technology (POSTECH) in June, 2008. He has worked on the synthesis of new nanostructured materials for energy and biological applications. He has published more than 45 papers in prominent international journals and has had more than 2450 citations.

vide an opportunity to understand the physical properties of one-dimensional (1D) semiconductor nanomaterials and pave the way for the realization of electrical, optical, and optoelectronic devices that employ nanowires/nanorods.

In this respect, to explore the novel properties of 1D semiconductor nanowires, various semiconductor nanowires have been synthesized through the colloidal synthetic method, the vapor–liquid–solid (VLS) method, the solution–liquid–solid (SLS) method, and the template-based synthetic method. In this microreview, we will focus on the synthesis of 1D semiconductor nanostructures using the various methods mentioned above. As an example of the application of 1D semiconductor nanostructures, their applications in photovoltaic devices will be briefly reviewed.

Colloidal Synthetic Method for Semiconductor Nanorods

After the first synthesis of semiconductor nanocrystals by Bawendi's group,[2] the colloidal synthesis of nanoparticles has been popularly employed to prepare various nanocrystals that exhibit electrical, optical, magnetic, and chemical properties. The colloidal synthetic method was pioneered to fabricate monodispersed particles by LaMer and his colleagues.[7] Through the colloidal synthetic method, 1D nanowires or nanorods have been synthesized. The key idea for the formation of monodispersed nanoparticles is the separation of nucleation and growth steps. To separate nucleation and growth steps and achieve homogeneous nucleation, two techniques have been typically employed: the "hot-injection" method[8] and the "heating-up" method.[9] In the "hot-injection" method, burst nucleation is induced by injecting organometallic precursors at high temperature, and a sharp decrease in monomer concentration causes nucleation to slow down. In the case of the "heating-up" method, the reaction solution is prepared at room temperature and slowly heated to high temperature. During heat treatment, monomers accumulate in the solution and burst nucleation occurs to generate seeds above the critical concentration. Further focus of growth and size produced monodispersed nanoparticles. By using this "heating-up" method, various 1D semiconductor nanorods with uniform diameter have been synthesized.

Hyeon's group synthesized uniform and quantum-sized nanorods from the oriented attachment process by employing the "heating-up" method.[3] ZnS adopts a cubic zincblende structure below 1020 °C, which leads to difficulty in synthesizing 1D ZnS nanorods with a cubic zincblende structure. Diethylzinc was employed as a precursor to synthesize rod-shaped ZnS nanorods and a solution that contained diethylzinc, sulfur, and hexadecylamine was aged at 300 °C. The initial product was a mixture of 80% rods and 20% spheres. Further aging at 60 °C in oleylamine generated ZnS nanorods with 5 nm diameter and 21 nm length. High-resolution transmission electron microscopy (HRTEM) revealed that the interplanar distance along the growth axis was 0.311 nm, which matched the interplanar spacing of the {111} plane of the cubic zincblende structure of ZnS (Figure 1, A). The synthesis of ZnS nanorods was achieved by the formation of ZnS short nanorods, followed by oriented attachment of ZnS nanocrystals during the second aging in oleylamine (Figure 1, B). Due to the cubic zincblende structure, 1D nanowires/nanorods of a cubic crystal structure are not easily synthesized. However, in this work, cubic ZnS nanords were synthesized by means of kinetic control and the oriented attachment mechanism. The authors claimed that the amine group selectively adsorbs to the {110} facet of ZnS nanocrystals and minimizes its energy, thereby leading to an enhancement of the surface-energy difference between the {110} and {111} facets. The oriented attachment of the remaining nanoparticles is caused by the dipole–dipole attraction of preformed ZnS nanocrystals.

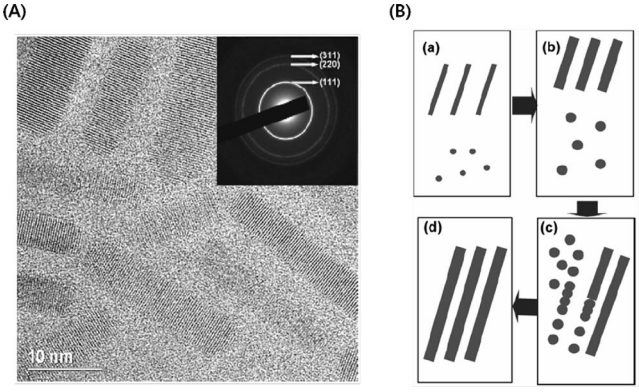

Figure 1. (A) High-resolution TEM image of ZnS nanorods. (inset) Electron diffraction pattern of ZnS nanorods. (B) Overall synthetic procedure for the nanorods: (a) Kinetic formation of short nanorods, (b) interparticle ripening, (c) oriented attachment of the 5 nm-sized quasispherical nanocrystals to form elongated nanorods, and (d) Ostwald ripening to form smooth-surfaced nanorods. Adapted from the literature.[3]

A 1D structure of n-type semiconductor oxide materials is quite useful for applications in photovoltaics and photocatalysis to enhance the electron-transport rate and achieve spatial separation of electrons and holes.

Titania (TiO_2) is an n-type semiconductor with a wide band gap (3.2 eV for anatase) and has been used in a variety of applications including solar cells, photovoltaic cells, and lithium-ion batteries. The single crystalline nanowire/rod-shaped TiO_2 has been favorable for facile transport of electrons when it was used as a photoanode of dye-sensitized solar cells. Joo et al.[10] reported large-scale synthesis of TiO_2 nanorods by means of nonhydrolytic sol–gel ester elimination reaction (Figure 2). In this colloidal approach, as a chemical reaction, they chose a nonhydrolytic sol–gel method to make TiO_2 nanorods. The nonhydrolytic sol–gel method can be applied to the synthetic systems in which addition of water should be completely avoided. In nonhydrolytic sol–gel processes, an alkyl halide elimination process in which metal alkoxide and metal halide react to form metal oxides is typically adopted. However, the titanium halide precursor has a highly acidic property and can react

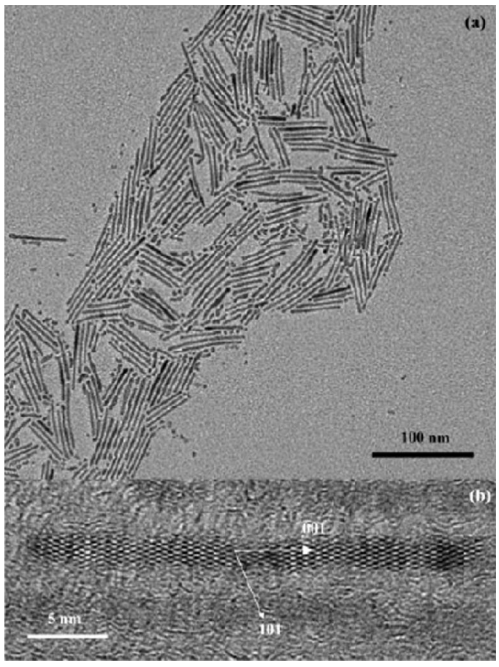

Figure 2. (a) TEM image of as-synthesized TiO_2 nanocrystals. (b) HRTEM image of TiO_2 nanorods. Adapted from the literature.[10]

vigorously with the Lewis base organic ligand. The strong Lewis acid–base interaction between metal chloride and organic ligand usually leads to an uncontrollable nonhydrolytic sol–gel reaction. To avoid this, they synthesized TiO_2 nanorods from a nonhydrolytic ester elimination reaction of titanium(IV) alkoxide and oleic acid; see Equations (1) and (2).

$$\equiv Ti(O\text{–}i Pr) + HOOC(CH_2)_7CH{=}CH(CH_2)_7CH_3 \rightarrow \equiv Ti\text{–}OH + (O\text{–}i Pr)C(=O)(CH_2)_7CH{=}CH(CH_2)_7CH_3 \quad (1)$$

$$\equiv Ti\text{–}OH + HO\text{–}Ti\equiv \rightarrow TiO_2 + H_2O \quad (2)$$

The mixture of titanium(IV) isopropoxide, oleic acid, and hexadecylamine was gradually heated to 270 °C for a period of 20 min and further aged at this temperature for 2 h to get TiO_2 nanorods. The as-synthesized product was mainly nanorods with a small amount of quasispherical particles. A size-selection process generated pure TiO_2 nanorods. The nanorods were grown along the [001] direction, which is evidenced by HRTEM images and the greater intensity of the (004) diffraction peak relative to that of the bulk. This is ascribed to the surface energy of the {001} surfaces that is 1.4 times higher relative to that of the {101} surfaces, as predicted by Donnay–Harker rules.[11] By changing the amount of hexadecylamine (HDA), the width of the nanorods was controlled from 2 to 3.5 nm because HDA selectively adsorbs onto the {101} surfaces. After removal of oleic acid on the nanorod surface by the reduction of the carboxylic group, the naked nanorods exhibited higher photocatalytic activity due to higher surface area, the large amount of hydroxy radicals and their larger band gap (3.33 eV), as compared with that of bulk anatase (3.2 eV).

The Vapor–Liquid–Solid (VLS) Synthetic Method for Semiconductor Nanowires

The VLS synthetic method was first proposed by Wagner et al.[12] in the 1960s. Since nanowires (solid) are grown in liquid droplets by absorbing vapor-phase precursors, this method is called vapor–liquid–solid. Relative to other vapor-phase methods, the VLS method has several advantages such as producing highly anisotropic single-crystalline structures, growth at a specific site with a uniform size, and relatively mild synthesis conditions. The process of the VLS method is schematized in part a of Figure 3. It can be classified into three stages: (i) metal alloying, (ii) crystal nucleation, and (iii) axial growth.

By using various lithographic or nonlithographic (by colloidal solution, galvanic displacement, and so on) techniques, patterned metal clusters can be prepared on the substrate. Each cluster acts as a catalyst site to grow nanowires. However, metal clusters should be changed to liquid droplets for preferential absorption of vapor precursors (which contain target materials) and nucleation of target materials. If the binary mixture of metal clusters and target materials is a eutectic mixture, liquid alloy droplets form when the temperature exceeds the eutectic point, and the melting temperature of a cluster is reduced significantly, as shown in Figure 3 (b).[13] For this reason, a process of alloying the metal and target materials (using vapor precursor or sub-

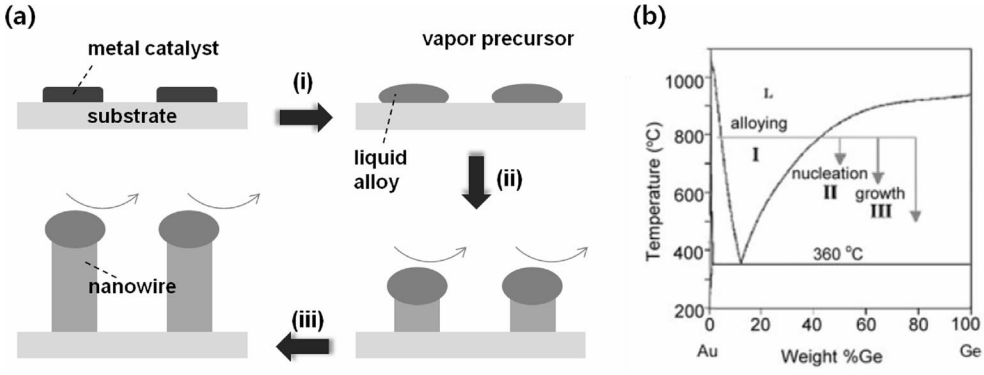

Figure 3. (a) Schematic illustration of the VLS growth process. (b) Au–Ge binary phase diagram. The three stages are projected onto the diagram to show the compositional and phase evolution during the nanowire growth process. The latter is adapted from the literature.[13]

strate) is first conducted. The vapor precursors are easily absorbed into the liquid alloy droplets due to a high sticking probability and a large accommodation coefficient of the surface of the liquid droplets.[14–16] Vapor precursors can be prepared by various methods (for example, chemical vapor deposition, laser ablation, thermal evaporation, electron beam evaporation, and so on), and the difference of methods would not significantly affect the quality of nanowires. Continued absorption of vapor precursors increases the concentration of target materials, so that the liquid droplets become supersaturated. When the concentration of target materials exceeds a certain level, crystal nucleation starts at the solid–liquid interface. Since less energy is required for nucleation at the solid–liquid interface, further dissolution of target materials induces unidirectional (axial) growth of nanowires at this interface. In the distant past, the only direct evidence for supporting the VLS process was an alloy droplet on the tip of a nanowire. However, in 2001, the VLS growth of Ge nanowires was directly observed by in situ TEM, and the validity of the above-described stages was demonstrated clearly.[13]

To successfully synthesize nanowires by the VLS method, several aspects need to be considered. Before carrying out an experiment, the proper selection of a metal catalyst constitutes one of the important steps. The selected metal should be able to form a eutectic mixture with the target material. The binary phase diagram can be utilized to confirm the eutectic composition and the range of required temperature to prepare the liquid alloy. Other essential properties that the metal catalyst must possess are its being inert to other materials and having a low vapor pressure at the growth temperature. To satisfy all these requirements, gold is the catalyst frequently used for the VLS method. Furthermore, the following conditions should be considered in controlling the growth of nanowires. The diameter of nanowires largely depends on the size of metal catalysts. In a study of Au-catalyzed Si nanowires by Wu and Yang,[13] a linear relationship was observed between the size of an Au cluster and the diameter of the nanowires. In general, small catalysts yield thin nanowires. The growth temperature and the amount of vapor precursors influence the supersaturation level of liquid droplets, which consequently affects the growth rate of nanowires. For the growth of unidirectional nanowires, a low supersaturation level is required to prevent secondary nucleation in liquid droplets. In addition, the crystal orientation of the substrate affects the growth orientation of nanowire arrays.[17,18] In a recent study, the presence of even a small amount of oxygen was found to influence the morphology of nanowires.[19]

Nanowires that consist of various inorganic materials have been synthesized by the VLS method. Among them, Si nanowires, the most important elemental semiconductor, have attracted much attention due to their potential applications in electronic and optoelectronic devices.[20–36] Therefore, many researchers have focused on this topic, and at present, the VLS method is generally utilized to fabricate Si nanowires. The most well-known growth procedure is the chemical-vapor deposition (CVD), which uses volatile vapor precursors (such as $SiCl_4$,[12,13,20,21] SiH_4,[22–25] and Si_2H_6[26,35]) with Au employed as the metal catalyst. The details of the growth conditions used in these experiments are somewhat different due to their dependence on the type of vapor precursors, the pressure of vapor, and other variables; however, all experiments follow the above-described procedure. The SEM image shown in the study of Yang's group is an example of Si nanowire arrays fabricated by CVD.[21] To synthesize these nanowires, a gas mixture of $SiCl_4$ and H_2 was used to supply the Si species to the catalyst. H_2 reduced $SiCl_4$ at a high temperature (900–950 °C), and Si nanowires were grown on an Au-coated Si(111) substrate. Unlike the above result, Akhtar et al.[26] reported that when Si_2H_6 was used as a vapor precursor, a relatively low temperature (350 °C) was required for growing high-density Si nanowires due to the low decomposition temperature of Si_2H_6. Recently, research has been conducted by Lee et al.[36] on the relationship between the VLS nanowire growth and the local temperature difference. In their study, a vertical temperature gradient was established on a substrate by means of the air circulation cooling applied below the substrate. They demonstrated that under this experimental condition, the growth direction and rate of nanowires follow the local temperature gradient and that instability of the temperature gradient induces the nanowires to grow in a random direction.

The laser ablation method is the another versatile method for the synthesis of Si nanowires.[27,28,34] Ablation of a mixed Si–catalyst target creates a vapor of Si and catalyst that subsequently condenses into liquid droplets with the same composition as that of the target. Then the growth of Si nanowires begins in these droplets when the catalysts become supersaturated with Si. Consequently, there is no need to use a substrate. A high-intensity laser easily evaporates the target materials, even those that have a high melting point. Moreover, this method produces a small size and large number of nanowires.[28] As an example, Yang et al.[34] described the synthesis of Si nanowires by the laser ablation method with various catalysts (Fe, Ru, Pr, and SiO_2). The resulting Si nanowires were single-crystalline with a range of core diameters (5–36 nm) and SiO_x sheath thicknesses (3–10 nm), depending on the type of the catalyst.

It is known that Au creates midgap defect states in Si; hence, Au is considered to be unsuitable for use in electronic devices.[29,30] To overcome this shortcoming, instead of Au, various metals have been studied as alternative metal catalysts.[29–33] Looking at some of the recent studies on this topic, Garnett et al.[29] reported that size-controlled epitaxial undoped or boron-doped Si nanowires were synthesized using Pt nanoparticles. The epitaxially oriented Si nanowires with an Al catalyst were fabricated by Ke et al.[32] It was confirmed that nanowires were P^+ doped with Al. They also demonstrated that high partial pressure of H_2 and SiH_4 led to a decrease in the Al oxidation and an increase in the growth rate of Si nanowires (Figure 4). Through the gas-phase reaction of $SiCl_4$ with Zn vapor, Uesawa et al.[33] obtained Si nanowires with a single step. They found that the growth temperature affected the dia-

meter and roughness of Si nanowires, and Zn served a reducing agent for $SiCl_4$ as well as a catalyst site for the growth of nanowires.

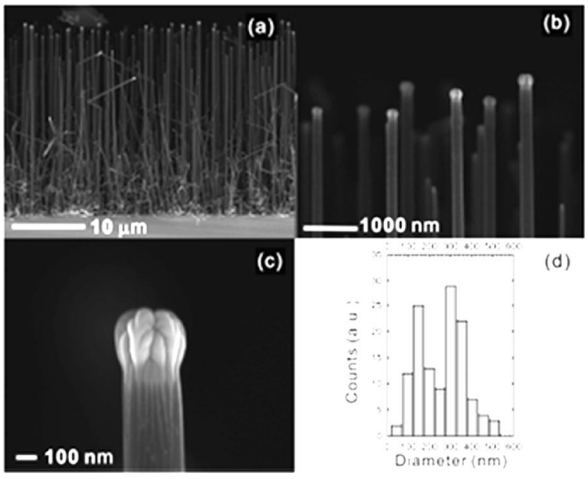

Figure 4. (a–c) Cross-sectional SEM images and (d) diameter distribution of Al-catalyzed Si nanowires grown at 550 °C, 100 Torr reactor pressure, and 6 Torr SiH_4 partial pressure. Adapted from the literature.[32]

Zinc oxide (ZnO), another attractive semiconductor, has a wide band gap (3.4 eV) and a large exciton binding energy (60 meV). With a view toward utilizing its remarkable optical properties and enhancing the physical and chemical properties, many researchers have studied ZnO nanowires.[17,37–45] In 2001, patterned single-crystalline ZnO nanowires were first synthesized by Yang's group.[17,37,38] The Zn and CO/CO_2 vapor generated by carbothermal reduction of ZnO powder acted as Zn and oxygen sources, respectively. Then, with the Au catalyst on Si substrates, the ZnO nanowires were synthesized by the VLS process (Figure 5). They also showed that nanowires could be aligned vertically with a sapphire substrate instead of an Si one. By using Cu as the catalyst, Li et al.[43] synthesized ZnO nanowires on a Cu-coated p-type Si(100) substrate. In that study, the diameters of ZnO nanowires could be controlled in a range 80–150 nm by controlling the thickness of the Cu film. They also employed the thermal annealing process to fabricate almost vertically grown ZnO nanowires on an Si substrate.

Following the above studies, well-aligned ZnO nanowires fabricated without the use a catalyst were reported in several papers.[39–41] To fabricate these nanowires, Geng et al.[40] created a steady-state vapor environment by means of a horizontal double-tube system, and Kar et al.[41] used oxygen-assisted thermal evaporation of metallic Zn powder. Both studies suggested that Zn and ZnO_x vapors condensed to liquid droplets on the substrate; these droplets acted as the catalyst sites. They called this process a "self-catalyzed VLS method." Recently, a new selective growth method was demonstrated using self-assembled Au nanoparticles by Ito et al.[42] The anchoring of functionalized Au nanoparticles to a patterned seed layer enabled the subsequent selective growth of ZnO nanowire arrays. Thus, this growth technique could eliminate the use of a patterned evaporated Au film and also vacuum-deposition processing.

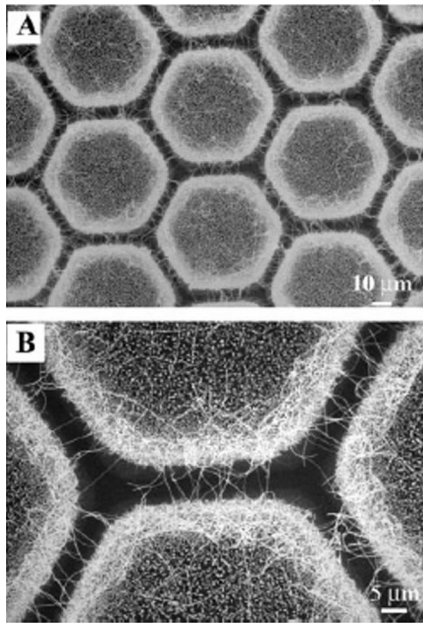

Figure 5. SEM images of a patterned ZnO nanowire network on Si substrate. Adapted from the literature.[17]

The Solution–Liquid–Solid (SLS) Synthetic Method for Semiconductor Nanowires

In 1995, Buhro's group reported a solution synthesis of crystalline III–V semiconductor nanowires at low temperature, and they first proposed the solution–liquid–solid (SLS) synthetic method.[46] As seen from the name of the method, the precursors are transported through the solution rather than a vapor phase, and the entire growth process of the SLS method is analogous to that of VLS (Figure 6). In the SLS synthetic method, organometallic precursors are used to supply desired elements to an organic solvent, and a metal with a low melting point acts as catalyst. The increased temperature of the solution leads to the formation of liquid-metal droplets, which catalyze the decom-

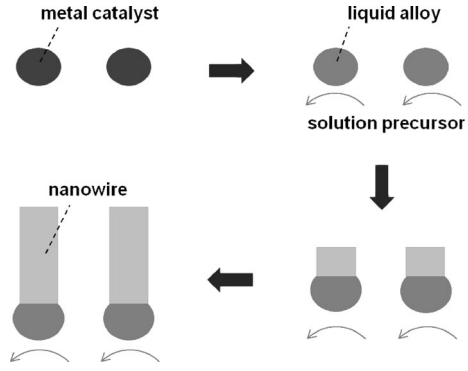

Figure 6. Schematic illustration of the SLS growth process.

position of the precursors. The desired elements dissolve into these droplets until supersaturation is attained. Then nucleation occurs and is followed by the growth of nanowires, as in the VLS method.

In comparison with the VLS method, the SLS method has several features that attract the interest of many researchers. The most important feature is that crystalline nanowires can be synthesized using a low-melting-point metal catalyst at a low growth temperature (<350 °C). This not only leads to less energy consumption, but is also useful for semiconductor processes that require a low temperature. Moreover, the nanowires fabricated using the SLS method usually have smaller diameters and exhibit stronger quantum confinement effects than those fabricated using the VLS method.[47,48] Further, in a solution-based system, it is possible to use a surfactant. By bonding it to the surface of nanowires, various properties of the nanowires can be controlled. First, the electric properties of nanowires, which are affected by abrupt surface termination, are improved by surface passivation. Steric stabilization by surfactant is another advantage. Furthermore, the dispersion of nanowires in an organic solvent is facilitated by the hydrophobic part of the surfactant, and nanowires can be rendered dispersible in an aqueous solvent by the ligand-exchange method.

As in the VLS method, in the SLS method, too, the diameter of nanowires largely depends on that of liquid-metal droplets. Therefore, to fabricate nanowires with a narrow diameter distribution, it is first necessary to preparing near-monodisperse nanoparticles of a metal catalyst. In addition, the metal catalyst must form liquid droplets at the reaction temperature. Solvation abilities and reactivities should also be considered when selecting a catalyst. The solubility of an element in the catalyst material is another factor that influences the selection of a catalyst. A material suitable for satisfying these conditions is a metal with a low melting point such as In, Sn, and Bi.[47] Apart from the above-mentioned factors, some experimental conditions (for example, the catalyst amount, concentration of reaction mixture, a type of surfactant, growth temperature) also affect the synthesis of nanowires.

Further, by using Au nanoparticles as the catalyst and diphenylsilane as the silicon precursor, Korgel's group synthesized crystalline Si nanowires with a narrow diameter distribution (4–5 nm) in the solution phase.[49] For preparing an Au–Si eutectic compound, a temperature higher than the boiling point of the solvent is required. Therefore, nanowires were synthesized in the supercritical solution phase. After the formation of Au–Si alloy, the further growth processes seemed very analogous to those in the case of the VLS or SLS method. From this result, they proposed the supercritical-fluid–liquid–solid (SFLS) synthetic method.[50] Although, as compared with the SLS method, the synthetic conditions of the SFLS method are somewhat hazardous due to its high temperature and pressure, it is possible to use the easily available smaller monodisperse metal nanoparticles, which have a high melting point. Because metal nanoparticles are protected by an organic monolayer, the size of nanoparticles is maintained even at the reaction temperature. Thus, by the SFLS method, very thin crystalline semiconductor nanowires can be synthesized with a narrow diameter distribution. In a recent paper, the electrically controlled solution–liquid–solid (EC-SLS) method was designed by Dorn et al.[51] By using this method, they reported the synthesis of CdSe and InP nanowires that were controllably grown between two electrodes.[51,52] This method facilitates the direct integration of solution processed nanowires into devices. Nanowire growth can be controlled by varying the voltage between electrodes. Furthermore, by measuring the conductivity across the electrodes, nanowires bridging the electrodes can be monitored. For these reasons, the EC-SLS method has potential to be applied to the fabrication of nanowire devices.

Ever since the SLS growth of crystalline III–V semiconductor nanowires was reported by Buhro's group,[46] related studies have been presented continuously.[53–59] In 2003, Yu and Buhro reported that GaAs nanowires with a narrow diameter distribution were obtained by using In nanoparticles.[53] Size-controlled and near-monodisperse In nanoparticles could be prepared by heterogeneous seeded growth.[54] It was the key factor in the synthesis of nanowires with a desired size distribution. In addition, a polymer surfactant that was contained in the reaction mixture stabilized the In nanoparticles and GaAs nanowires. This rendered the nanowires dispersible in an organic solvent. In a similar manner, InP nanowires that were dispersible in an organic solvent were grown.[55] Further, Fanfair and Korgel synthesized GaP, GaAs, InP, and InAs nanowires by using Bi nanoparticles as the catalyst.[56] To prepare pure Bi nanoparticles, they used Bi^{III} 2-ethylhexanoate without employing Au nanocrystals, which acted as heterogeneous seeds. InAs and GaP nanowires were obtained successfully in the trioctylphosphane oxide/tri-*n*-octylphosphane (TOPO/TOP) solvents system. Although InP nanowires exhibited some stacking faults, they were obtained in a high yield. However, in the case of GaAs, use of trioctylamine instead of TOPO/TOP as the solvent led to high-quality nanowires in a high yield. In addition, for the purpose of facilitating comparisons with InP quantum dots, Wang et al.[47] synthesized InP nanowires that were stabilized by surfactants typically used in quantum-dot synthesis. The reaction system consisted of indium myristate and tris(trimethylsilyl)phosphane, which served as the precursor; polydecene, which was used as the solvent; Bi nanoparticles, which acted as the catalyst; and several surfactants. The surfactants used in this procedure were *n*-hexadecylamine (HDA), TOPO, TOP, *n*-octylphosphonic acid (OPA), and di-*n*-octylamine (DOA). Each surfactant played an important role; HDA improved the nanowire crystallinity and affected the diameter distribution. TOPO and TOP reduced the number of kink sites. OPA quenched the homogeneous nucleation of InP-rod clusters, and DOA prevented the aggregation of Bi nanoparticles. The InP nanowires synthesized with these surfactants had a controlled diameter in the range of 4–12 nm with a narrow diameter distribution.

In addition to III–V semiconductor nanowires, the SLS growth of II–VI semiconductor nanowires has also been reported by many researchers.[60–65] Crystalline CdSe nanowires with a narrow diameter distribution were reported by Buhro's group in 2003.[60] By using near-monodisperse Bi nanoparticles as the catalyst, the CdSe nanowires were synthesized from cadmium stearate and n-R_3PSe (R = butyl or octyl) in TOPO at 240–300 °C. The diameter of nanowires was controlled by controlling the size of Bi nanoparticles and the reaction temperature. From these procedures, they obtained crystalline CdSe nanowires with a diameter of 5–20 nm. Grebinski et al.[61] reported the synthesis of CdSe nanowires by using Au/Bi catalyst nanoparticles. In this synthesis, CdO and TOPSe were used as precursors, and the Cd-coordinating surfactant was octanoic acid, which provides good control over the growth kinetics of nanowires. In addition to straight nanowires, branched (v-shaped, y-shaped, and tripod morphologies) nanowires were also synthesized by varying the Cd/Se precursor ratio and the excess amount of the TOP ligand. All of resulting crystalline nanowires had diameters below 10 nm with lengths of 1–10 μm and exhibited quantum confinement effects in their UV/Vis absorption spectra. In 2006, Wang et al.[47] synthesized several semiconductor nanowires, InP (described above), InAs, GaAs, CdSe, CdTe, and ZnTe by the SLS method. Among them, by using Bi nanoparticles, CdTe nanowires were obtained from the reaction of cadmium alkylphosphonate with CdO in the distilled TOPO solvent. To prevent a side reaction, cadmium alkylphosphonate was used instead of cadmium carboxylates. In a similar manner, ZnTe nanowires were synthesized by using zinc stearate and tri-*n*-butylphosphane telluride (TBPTe) as the precursor, 1-octadecene as the solvent, and TOP as the surfactant. Owing to their unique photonic and electrical properties, heterostructure nanowires have attracted considerable attention in recent years. SLS-grown CdS/CdSe heterostructure nanowires and their characterization were reported by Ouyang et al.[62] In this experiment, Bi nanoparticles were used as the catalyst, which is suitable for the growth of both CdS and CdSe components under similar reaction conditions. As shown in Figure 7, a substrate covered with Bi nanoparticles was loaded into the reaction solution, thus resulting in nanowires grown thereon. The substrate was then transferred to another reaction solution so as to grow heterostructure nanowires. In this manner, CdS/CdSe nanowires were synthesized with controlled sequences. Before long, ZnSe/ZnTe heterostructure nanowires were also successfully grown by the SLS method.[63] ZnTe nanowires were obtained from zinc stearate and TBPTe, first. After purification of the as-synthesized nanowires, ZnSe segments were grown on the ZnTe nanowire by using TOPSe and zinc stearate. The resulting ZnSe/ZnTe nanowires exhibited a quantum confinement effect due to their small diameter. In addition, from a series of experiments, it was found that the growth sequence and a complete removal of the unwanted precursor are quite important factors for obtaining ZnSe/ZnTe nanowires.

The Template-Based Synthetic Method for Semiconductor Nanowires

Template-based synthesis is one of the facile and versatile methods for the fabrication of nanowires. The overall process of this method is relatively simple. This method employs a template as a scaffold for guiding the growth. By filling or covering the template with a precursor, nanowires of desired materials can be generated. The resulting nanowires are then separated from the template by a posts-ynthetic treatment. As can be seen, the template-based method provides a simple and cost-effective route. In addition, various materials, such as polymer, metal, semiconductor, and carbon can be synthesized in the form of nanowires with a desired pattern and geometry. Although this method has a drawback that it is difficult to obtain single-crystalline nanowires, numerous studies have so far been conducted using this method for these reasons.

In the template-based method, depending on the type of a template used and the method used to deposit materials, a variety of approaches exist for the synthesis of nanowires. First, we describe the types of templates. Typical templates are made of porous material, mesostructures self-assembled from surfactants, nanowires, and so on. Among them, porous materials are most frequently used. Figure 8 shows the formation of nanowires and nanotubes from porous material. Channels within the porous material are actually the role of host. It should be considered that the precursor can wet the pores sufficiently and the pores can be blocked during the reaction.[66] Various deposition methods are used to load the precursor into the pores. Track-etched polycarbon-

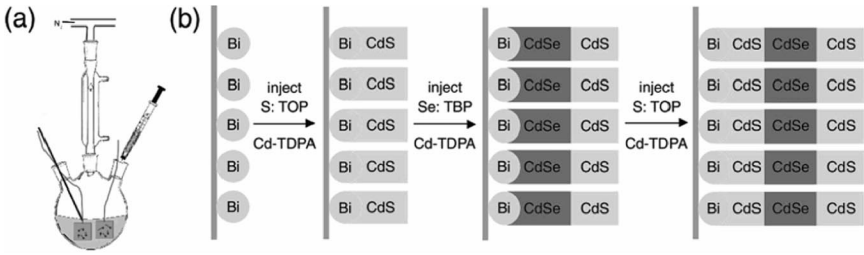

Figure 7. Synthesis of axial nanowire heterostructures. (a) Schematic of the solution reaction setup. (b) Bi nanocrystal catalysts nucleate and direct 1D nanowire heterostructure growth with the catalysts remaining at the terminus of the nanowires. Adopted from the literature.[62]

ate membranes and anodic aluminum oxide (AAO) membranes are commonly used porous materials. The former are made by heavy-ion bombardment and subsequent chemical etching. These membranes are available with a wide range of pore diameters, between 10 and 2000 nm, and can be easily dissolved in a particular solution so as to separate the as-synthesized nanowires. AAO membranes are obtained by anodic oxidation of aluminum in sulfuric, oxalic, or phosphoric acid solution.[66] Unlike track-etched membranes, AAO membranes have a nonintersecting pore structure with uniform cylindrical pores.[67] These membranes are also easily removed from nanowires after synthesis. The examples of using both membranes will be described below in more detail. In addition to these membranes, mesoporous materials have also been occasionally used as templates due to their small pore size.

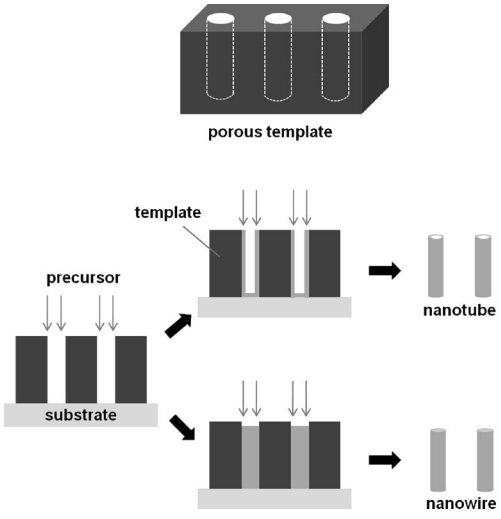

Figure 8. Schematic illustration of the formation of nanowires or nanotubes from a porous template.

Figure 9 shows the formation of nanowires by using self-assembled surfactant as a template.[68] Whereas porous materials serve as hard templates, these surfactants serve as soft templates. When the concentration of a surfactant exceeds the critical micelle concentration (CMC), cylindrical micelles are formed.[69] These micelles can then be used as a template. Through the specific chemical interaction between the micelles and the precursors, desired nanowires can be synthesized. To obtain pure nanowires, the surfactant is finally removed. Rao et al.[70] showed that CdS and CdSe nanowires were successfully synthesized by using surfactants such as *t*-octyl-$(OCH_2CH_2)_xOH$ (x = 9, 10; Triton-X), and sodium bis(2-ethylhexyl) sulfosuccinate (AOT). After obtaining the as-synthesized nanowires, cyclohexane and diethyl ether could remove the residual surfactant in the washing process. In that paper, nanotubes were also obtained by changing the surfactant concentration. In a similar manner, ZnSe nanorods were synthesized using sodium laurylsulfonate (SDS) and AOT micelle as the template.[71] Furthermore, the synthesis of PbSe nanowires in a mixture of arachidic acid and octadecylamine was also reported by Liu et al.[72]

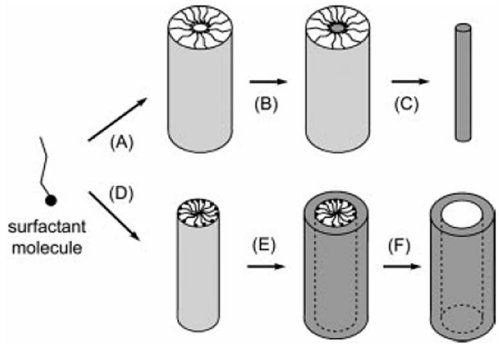

Figure 9. Schematic illustrations that show the formation of nanowires by templating against mesostructures self-assembled from surfactant molecules: (A) formation of a cylindrical micelle; (B) formation of the desired material in the aqueous phase encapsulated by the cylindrical micelle; and (C) removal of the surfactant molecules with an appropriate solvent (or by calcination) to obtain an individual nanowire. (D–F) Similar to the processes illustrated in (A–C), except that the exterior surface of an inverted micelle serves as the physical template. Adapted from the literature.[68]

Nanowires can themselves play the role of a template. Such a template can be used to produce coaxial nanocables. Yin et al.[73] synthesized silver/silica coaxial nanocables in this manner. They also showed that silica nanotubes could be obtained by selective dissolution of the silver core. On the other hand, by reaction with a precursor, nanowire templates can be directly converted to new ones. Several studies have demonstrated that through topotactic transformation, trigonal Se nanowires were converted to Ag_2Se nanowires without changing the single crystallinity.[74–76] From the resulting Ag_2Se nanowires, CdSe nanowires were obtained by cationic exchange reaction.[77] In a recent paper, Park et al.[78] described that, through the formation of ZnCdTe-CdTe coaxial structure as an intermediate, ZnTe nanowires were transformed into CdTe nanowires. The transformation of Ag_2Te nanowires into CdTe, ZnTd, and PbTe nanowires was also presented by Moon et al.[79]

As mentioned above, the method used to deposit a material is also important in the synthesis of nanowires. Several deposition methods are commonly used to obtain nanowires, such as electrochemical deposition, electroless deposition, chemical polymerization, sol–gel deposition, and chemical-vapor deposition.[66] Accordingly, if we consider the templates together, there exist various synthetic routes, all of which cannot be dealt with in this part. Hence, next, we only briefly describe electrochemical deposition with a porous template and its application to the fabrication of semiconductor nanowires. Further details can be obtained from some references.[66,67,80,81]

Figure 10 is the schematic illustration of typical electrochemical deposition with a porous template.[80] A conductive layer, which serves as a working electrode, is prepared with ion sputtering or thermal evaporation of metal on one side of the template. The template is subsequently immersed in the reaction solution that contains desired material precursors. Application of a potential with a counter electrode enables electrochemical deposition within the channels of

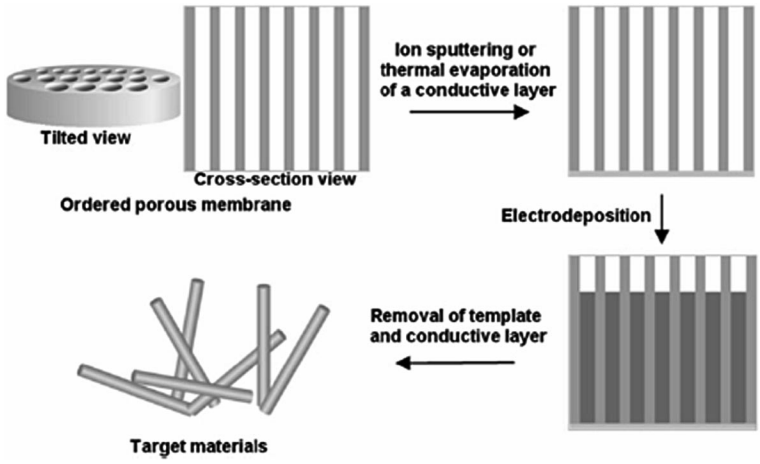

Figure 10. Schematic of the electrosynthesis of nanomaterials within a template that contains cylindrical pores. Adapted from the literature.[80]

the template. By removal of the template and conductive layer, the target materials are obtained. This deposition method has several noteworthy advantages, such as mild reaction conditions, relatively high growth rate, and easily tunable dimensions of nanowires. Therefore, this method has been widely used to form metal, semiconductor, and conducting polymer nanowires.

Mentioned below are several studies on the application of electrochemical deposition with porous templates for the fabrication of semiconductor nanowires. In 1996, Routkevitch et al.[82] reported the use of electrochemical deposition based on single-step AC electrolysis for fabricating CdS nanowires with a diameter as small as 9 nm. AAO membranes were used as the porous template. $CdCl_2$ and elemental sulfur dissolved in dimethyl sulfoxide were contained in the electrolyte. In addition, it was shown that the pore diameters and densities of the AAO membranes could be easily controlled by changing the anodization parameters such as the electrolyte used, its concentration, and the anodizing voltage. By using a cyclic voltammetric technique for CdSe deposition with AAO or track-etched polycarbonate membranes, Peña et al.[83] synthesized CdSe nanowires sandwiched between Au or Ni metal segments. Almost at the same time, large-scale uniform ZnO nanowires were synthesized with AAO membranes by using the DC electrochemical deposition technique.[84] ZnTe nanowires were also successfully synthesized by pulsed electrochemical deposition into AAO membranes.[85] In a recent paper, Mallet et al.[86] reported the fabrication of Si nanowires by electrochemical deposition with a polycarbonate membrane. Because the reduction potential of a solvent must be higher than that of the deposit material, they used a nonaqueous solvent. Due to the use of a nonaqueous system, the oxidation of Si also could be prevented. The resulting Si nanowires were composed of pure amorphous silicon and had a precisely controlled diameter. Mallet et al.[86] also showed that annealing treatment in an argon atmosphere induced the crystallization of Si nanowires without causing a morphology change.

Recently, epitaxially grown Si nanowires have been prepared with the VLS method by using an AAO membrane template.[87,88] Lombardi et al.[87] synthesized vertically aligned epitaxial Si nanowires on an Si(111) substrate in this manner. They first deposited patterned Au clusters onto a substrate with AAO membranes. After removing the AAO membranes, Si nanowires were grown using the $SiCl_4$ vapor precursor. Therefore, without using lithographic techniques, this approach allowed the epitaxial growth of vertical nanowires with a narrow diameter distribution and a high packing density. On the other hand, in a study by Shimizu and co-workers,[88] AAO membranes were used until the completion of the VLS growth. This refined not only the Au cluster pattern but also the orientation of nanowires. Accordingly, in spite of nonpreferential orientation in a general case, epitaxial Si(100) nanowires could be obtained on a Si(100) substrate. Figure 11 shows a schematic illustration of the growth of Si nanowires. As shown in this illustration, the removal of SiO_2 prior to the deposition of Au clusters was another crucial step for the epitaxial growth of Si nanowires. This indicated the importance of direct contact between the Au clusters and the Si substrate for the realization of epitaxial growth.

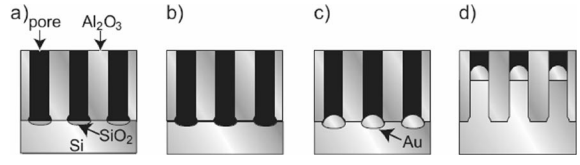

Figure 11. Schematic illustration of the growth of Si nanowires in an AAO template using Au nanoparticles as the catalyst: (a) after pre-annealing at 900 °C, (b) after HF etching to remove SiO_2, (c) electroless Au deposition, and (d) VLS growth of Si nanowires. Adapted from the literature.[88]

Application of 1D Nanowires/Nanorods to Photovoltaics

Organic–Inorganic Hybrid Solar Cells

Photovoltaic devices were fabricated from blends of branched CdSe nanorods synthesized by Peng and Peng[89] and a conjugated polymer.[90] CdSe branched nanorods act as good electron acceptors from the conjugated polymer poly[2-methoxy-5-(3′,7′-dimethyloctyloxy)-*p*-phenylenevinylene] (OC_1C_{10}-PPV). The photovoltaic performance of the branched CdSe (50 nm long and 5 nm thick) conjugated polymer composite was compared with the nanorod CdSe (65 nm long and 5 nm thick) conjugated polymer composite. The fabricated photovoltaic device is shown in Figure 12. The mixed solution that contained CdSe and conjugated polymer was spin-coated onto the surface of poly(3,4-ethylenedioxythiophene)/poly(styrenesulfonate) (PEDOT/PSS). The external quantum efficiency (EQE) of the branched nanorod system was 45% under 0.39 mW cm^{-2} illumination at 480 nm, whereas an EQE of 23% was obtained with CdSe nanorods. This improved efficiency was derived from improved electron transport. Under illumination at AM 1.5 global conditions (G), the solar-power conversion efficiency was 1.8%, slightly higher than that of poly(3-hexylthiophene)/nanorod devices.[91]

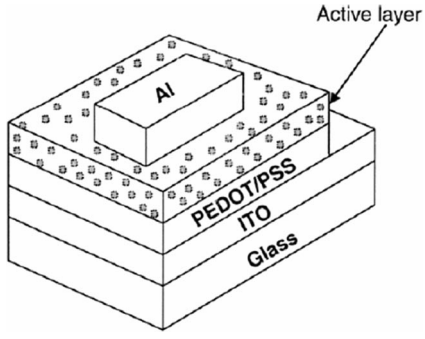

Figure 12. Photovoltaic device structure. Adapted from the literature.[90]

All-Inorganic Solar Cells

An ultrathin donor–acceptor solar cell composed entirely of inorganic nanocrystals was developed by Alivisatos' group.[92] In the case of polymer solar cells, the electron transport can be improved by employing inorganic nanocrystals. However, due to their organic phase, the stability and electron mobility were limited. To improve the air stability and electron mobility, all-inorganic solar cells with donor–acceptor (D–A) heterojunctions were fabricated that employed CdTe nanorods as the donor and CdSe nanorods as the acceptor. Staggered energy levels were achieved by the band alignment of the nanorods of these two different semiconductors. To fabricate D–A heterojunctions, CdTe and CdSe were sequentially spin-coated on indium tin oxide (ITO) glass; this was followed by the deposition of aluminum as a reflective top contact (Figure 13, a). By exposing the films to full-sun irradiation, a marked increase in conductivity was observed, which indicates that these semiconductor D–A type solar cells have an extremely limited number of untrapped carriers in the dark, similar to organic solar cells. Directed diffusion, as dictated by type-II heterojunctions, acts as the driving force for carrier extraction. The resulting solar cell exhibited a power-conversion efficiency of 2.9% under simulated AM 1.5 G illumination and was insensitive to the photo-oxidation characteristic of organic-based devices. After open-circuit exposure to the ambient atmosphere and lighting for 13000 hours, the cell exhibited a 13.6% increase in its efficiency (Figure 13, b). This exceptional stability indicates the robustness of such D–A type all-inorganic solar cells over their organic counterparts.

Metal–Oxide Nanowires as Photoanodes for Solar Cells

Yang's group employed a dense array of oriented, crystalline ZnO nanowires as n-type semiconductors of dye-sensitized solar cells (DSSCs).[93] Typically for DSSCs, thick films (≈10 μm) of n-type semiconductor metal oxides have been employed. Electron collection injected into a conduc-

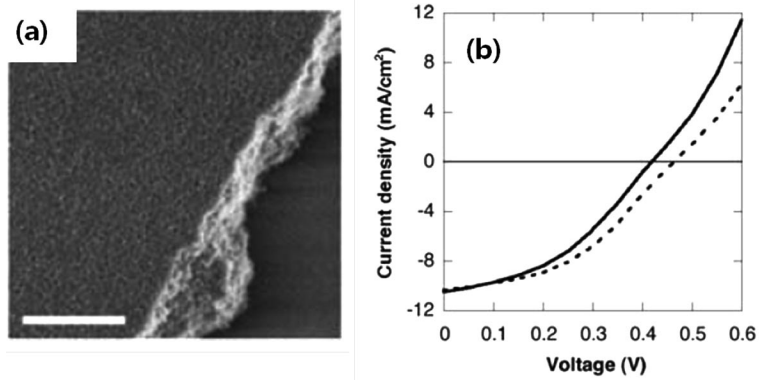

Figure 13. (a) Scanning electron micrograph (SEM) image of typical spin-cast film of colloidal nanocrystals. (b) Current–voltage behavior at simulated one-sun AM 1.5 G illumination for a typical sintered bilayer device upon first exposure to air (solid) and after 13000 hours of exposure to ambient atmosphere and light under open-circuit conditions. Adapted from the literature.[92]

tion band of n-type semiconductors is one important issue in achieving high conversion efficiency of DSSCs. To improve the absorption of red and infrared light, the nanoparticular photoanode film can be thickened to exceed the electron diffusion length through the nanoparticle network. It solves the problem of increasing the electron diffusion length in the photoanode by replacing nanoparticular films with an array of oriented single-crystalline nanowires. Arrayed ZnO nanowires were synthesized in aqueous solution using a seeded growth process.[94] Nanowires were grown from ZnO quantum dots onto F:SnO_2 (FTO) conductive glass substrates through the thermal decomposition of a zinc complex. By using the Einstein relation, $D = k_BT\mu/e$ in which k_B is the Boltzmann constant, T is the temperature, and μ is mobility of electrons, an electron diffusivity D_n = 0.05–0.5 $cm^2 s^{-1}$ was obtained, and this value is several hundred times larger than the highest reported diffusivity for TiO_2 and ZnO nanoparticle films in operating cells. The device showed a full Sun efficiency of 1.5%. The enhanced electron-transport property of 1D nanowires could greatly improve solar-cell conversion efficiency if the diameter of ZnO nanowires were reduced.

Sung et al.[95] employed TiO_2 nanorods, synthesized from the necking of truncated nanoparticles, by applying the synthesis of an "oriented attachment approach" as components for photoanode in DSSC. The nanorod structure decreased the intercrystalline contacts between grain boundaries and stretched the grown structure to impart it a specific directionality, which led to an improvement in the charge-collection efficiency due to a favorable electron-transport rate (Figure 14). The nanorod-based DSSC exhibits significantly enhanced J_{sc} due to improved charge-transport characteristics, and this was confirmed by measuring the J–V curves in the dark state and by stepped light-induced transient measurements of photocurrent and voltage (SLIM-PCV). The dark current onset of the nanorod-based DSSC was shifted to a higher potential range (0.47 V) relative to that of the nanoparticle-based DSSC (0.4 V), thus implying that the extent of charge recombination was reduced in the nanorod-based DSSC. The electron diffusion coefficients (D) and lifetimes (τ) of the nanoparticle- and nanorod-based DSSCs as a function of J_{sc} were analyzed by SLIM-PCV. The D value of a nanorod film is slightly higher than that of a nanoparticle film, thereby indicating that electron transfer is faster in nanoparticle films. This slight improvement resulted from the necking of nanoparticles and an increase in the average crystallite size. The electron lifetime (τ) was also increased when nanorods were employed as photoanodes in DSSCs. Because of the electron loss between the grain boundaries, the average electron diffusion length (L) of a nanorod film was much higher than that of an nanoparticle film due to increased D and τ. The resulting nanorod-based DSSC exhibited an enhanced efficiency of 6.2%, as compared with the nanoparticle-based DSSC (an efficiency of 4.3%).

Single-crystalline ZnO nanowires are combined with CdSe semiconductor nanocrystals (or quantum dots) so as to demonstrate a new type of quantum-dot-sensitized solar cell (QDSSC).[96] Instead of photosensitive dyes, semiconductor nanocrystals known as quantum dots have been combined with a mesoscopic network of TiO_2 nanoparticles to construct QDSSC.[97,98] A quantum dot (QD) has been known to generate multiple electron-hole pairs per photon, which could improve the efficiency of the device. For this reason, Norris' group employed QDs (CdSe nanocrystals) as a sensitizer and single-crystalline ZnO wire array as a photoanode.

The bright-field TEM image of CdSe/ZnO indicates that ZnO nanowires are decorated with an ensemble of CdSe QDs, and the QDs that are visible as circular dark spots are confirmed by the energy-dispersive X-ray (EDX) spectra. To check whether or not the optical absorption properties of CdSe QDs were preserved when they were assembled on the surface of ZnO nanowires, optical absorption spectra were obtained from diffuse reflectance measurements before and after the adsorption of QDs on the ZnO nanowires. After the adsorption of QDs on the surface of ZnO nanowires, features appeared at 465, 526, and 562 nm, which is typical for about 3 nm CdSe QDs. The absorption shape is identical to that observed in the absorption spectrum of about 3 nm free CdSe nanocrystals dispersed in methanol. This hybrid CdSe/ZnO was illuminated with the AM 1.5 spectrum; The power-conversion efficiency and the short-circuit current of these QDSSCs assembled on the nanowires were 0.4% and 2.1 mA cm^{-2}. This study demonstrates the potential application of QDs as photosensitizers instead of using dyes coupled with one-dimensional n-type metal–oxide nanowires.

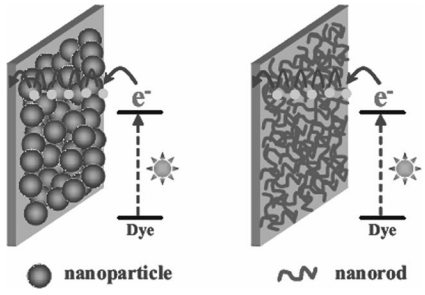

Figure 14. Simple representation of TiO_2 nanoparticle- and nanorod-based photoanodes on an FTO-coated glass substrate. Adapted from the literature.[95]

Conclusion and Outlook

Various synthetic methods have been used to synthesize a variety of 1D nanowires/nanorods. The colloidal method allowed synthesis of 1D semiconductor nanorods/nanowires through kinetic control, oriented attachment, and stabilizing specific surfaces using organic ligands. By the VLS method, Si and ZnO 1D structures can be synthesized by using Au as a catalyst and the resulting nanowires typically have single-crystalline structures. The entire growth process of the SLS method is analogous to that of VLS except the precursors are transported through the

solution rather than a vapor phase. By the SLS method, various kinds of III–V semiconductor and II–VI semiconductor nanowires have been synthesized with a narrow diameter distribution. Various templates including anodic aluminum oxides (AAO) and self-assembled surfactants have been adopted to grow semiconductor nanowires. Due to facile electron transport in 1D nanowires, they have been used as components of photovoltaic devices and enhanced photovoltaic properties have been shown. Future research will be directed toward the synthesis of new nanorods/nanowires that have potential applications in energy- and biology-related devices.

Acknowledgments

This research was supported by the Basic Science Research Program through the National Research Foundation of Korea (NRF) funded by the Ministry of Education, Science and Technology (KRF-20080-313-D00248). This research was further supported by National Research Foundation of Korea Grant funded by the Korean Government (2009-0071235) and by the grant from the Industrial Source Technology Development Programs (10033093) of the Ministry of Knowledge Economy (MKE) of Korea.

[1] J. Park, J. Joo, S. G. Kwon, Y. Jang, T. Hyeon, *Angew. Chem. Int. Ed.* **2007**, *46*, 4630–4660.
[2] C. B. Murray, D. J. Norris, M. G. Bawendi, *J. Am. Chem. Soc.* **1993**, *115*, 8706–8715.
[3] J. H. Yu, J. Joo, H. M. Park, S. I. Baik, Y. W. Kim, S. C. Kim, T. Hyeon, *J. Am. Chem. Soc.* **2005**, *127*, 5662–5670.
[4] D. V. Talapin, A. L. Rogach, E. V. Shevchenko, A. Kornowski, M. Haase, H. Weller, *J. Am. Chem. Soc.* **2002**, *124*, 5782–5790.
[5] X. Peng, J. Wickham, A. P. Alivisatos, *J. Am. Chem. Soc.* **1998**, *120*, 5343–5344.
[6] D. V. Talapin, A. L. Rogach, A. Kornowski, M. Haase, H. Weller, *Nano Lett.* **2001**, *1*, 207–211.
[7] T. Sugimoto, *Adv. Colloid Interf. Sci.* **1987**, *28*, 65–108.
[8] N. R. Jana, X. Peng, *J. Am. Chem. Soc.* **2003**, *125*, 14280–14281.
[9] J. Park, K. An, Y. Hwang, J. G. Park, H. J. Noh, J. Y. Kim, J. H. Park, N. M. Hwang, T. Hyeon, *Nat. Mater.* **2004**, *3*, 891–895.
[10] J. Joo, S. G. Kwon, T. Yu, M. Cho, J. Lee, J. Yoon, T. Hyeon, *J. Phys. Chem. B* **2005**, *109*, 15297–15302.
[11] J. D. H. Donnay, D. Harker, *Am. Mineral* **1937**, *22*, 446–467.
[12] R. S. Wagner, W. Ellis, *Appl. Phys. Lett.* **1964**, *4*, 89.
[13] Y. Wu, P. Yang, *J. Am. Chem. Soc.* **2001**, *123*, 3165–3166.
[14] H. J. Fan, P. Werner, M. Zacharias, *Small* **2006**, *2*, 700–717.
[15] C. N. R. Rao, F. L. Deepak, G. Gundiah, A. Govindaraj, *Prog. Solid State Chem.* **2003**, *31*, 5–147.
[16] B. A. Wacaser, K. A. Dick, J. Johansson, M. T. Borgstrom, K. Deppert, L. Samuelson, *Adv. Mater.* **2009**, *21*, 153–165.
[17] P. Yang, H. Yan, S. Mao, R. Russo, J. Johnson, R. Saykally, N. Morris, J. Pham, R. He, H. J. Choi, *Adv. Funct. Mater.* **2002**, *12*, 323–331.
[18] S. Ge, K. Jiang, X. Lu, Y. Chen, R. Wang, S. Fan, *Adv. Mater.* **2005**, *17*, 56–61.
[19] S. Kodambaka, J. B. Hannon, R. M. Tromp, F. M. Ross, *Nano Lett.* **2006**, *6*, 1292–1296.
[20] Y. Wu, R. Fan, P. Yang, *Nano Lett.* **2002**, *2*, 83–86.
[21] R. Fan, Y. Wu, D. Li, M. Yue, A. Majumdar, P. Yang, *J. Am. Chem. Soc.* **2003**, *125*, 5254–5255.
[22] K. K. Lew, L. Pan, E. C. Dickey, J. M. Redwing, *Adv. Mater.* **2003**, *15*, 2073–2076.
[23] Y. Wu, Y. Cui, L. Huynh, C. J. Barrelet, D. C. Bell, C. M. Lieber, *Nano Lett.* **2004**, *4*, 433–436.
[24] Y. Zhu, F. Xu, Q. Qin, W. Y. Fung, W. Lu, *Nano Lett.* **2009**, *9*, 3934–3939.
[25] A. Colli, A. Fasoli, P. Beecher, P. Servati, S. Pisana, Y. Fu, A. J. Flewitt, W. I. Milne, J. Robertson, C. Ducati, S. De Franceschi, S. Hofmann, A. C. Ferrari, *J. Appl. Phys.* **2007**, *102*, 034302.
[26] S. Akhtar, K. Usami, Y. Tsuchiya, H. Mizuta, S. Oda, *Appl. Phys. Express* **2008**, *1*, 014003.
[27] A. M. Morales, C. M. Lieber, *Science* **1998**, *279*, 208–211.
[28] J. Hu, T. W. Odom, C. M. Lieber, *Acc. Chem. Res.* **1999**, *32*, 435–445.
[29] E. C. Garnett, W. Liang, P. Yang, *Adv. Mater.* **2007**, *19*, 2946–2950.
[30] V. Schmidt, J. V. Wittemann, S. Senz, U. Gosele, *Adv. Mater.* **2009**, *21*, 2681–2702.
[31] S. Barth, F. Hernandez-Ramirez, J. D. Holmes, A. Romano-Rodriguez, *Prog. Mater. Sci.* **2010**, *55*, 563–627.
[32] Y. Ke, X. Weng, J. M. Redwing, C. M. Eichfeld, T. R. Swisher, S. E. Mohney, Y. M. Habib, *Nano Lett.* **2009**, *9*, 4494–4499.
[33] N. Uesawa, S. Inasawa, Y. Tsuji, Y. Yamaguchi, *J. Phys. Chem. C* **2010**, *114*, 4291–4296.
[34] Y. H. Yang, S. J. Wu, H. S. Chiu, P. I. Lin, Y. T. Chen, *J. Phys. Chem. B* **2004**, *108*, 846–852.
[35] J. B. Hannon, S. Kodambaka, F. M. Ross, R. M. Tromp, *Nature* **2006**, *440*, 69–71.
[36] G. Lee, Y. S. Woo, J. E. Yang, D. Lee, C. J. Kim, M. H. Jo, *Angew. Chem. Int. Ed.* **2009**, *48*, 7366–7370.
[37] M. H. Huang, Y. Wu, H. Feick, N. Tran, E. Weber, P. Yang, *Adv. Mater.* **2001**, *13*, 113–116.
[38] M. H. Huang, S. Mao, H. Feick, H. Yan, Y. Wu, H. Kind, E. Weber, R. Russo, P. Yang, *Science* **2001**, *292*, 1897–1899.
[39] L. Wang, X. Zhang, S. Zhao, G. Zhou, Y. Zhou, J. Qi, *Appl. Phys. Lett.* **2005**, *86*, 024108.
[40] C. Geng, Y. Jiang, Y. Yao, X. Meng, J. A. Zapien, C. S. Lee, Y. Lifshitz, S. T. Lee, *Adv. Funct. Mater.* **2004**, *14*, 589–594.
[41] S. Kar, B. N. Pal, S. Chaudhuri, D. Chakravorty, *J. Phys. Chem. B* **2006**, *110*, 4605–4611.
[42] D. Ito, M. L. Jespersen, J. E. Hutchison, *ACS Nano* **2008**, *2*, 2001–2006.
[43] S. Y. Li, C. Y. Lee, T. Y. Tseng, *J. Cryst. Growth* **2003**, *247*, 357–362.
[44] N. Kouklin, *Adv. Mater.* **2008**, *20*, 2190–2194.
[45] A. N. Red′kin, Z. I. Makovei, A. N. Gruzintsev, E. E. Yakimov, O. V. Kononenko, A. A. Firsov, *Inorg. Mater.* **2009**, *45*, 1246–1251.
[46] T. J. Trentler, K. M. Hickman, S. C. Goel, A. M. Viano, P. C. Gibbons, W. E. Buhro, *Science* **1995**, *270*, 1791–1794.
[47] F. Wang, A. Dong, J. Sun, R. Tang, H. Yu, W. E. Buhro, *Inorg. Chem.* **2006**, *45*, 7511–7521.
[48] M. Kuno, *Phys. Chem. Chem. Phys.* **2008**, *10*, 620–639.
[49] J. D. Holmes, K. P. Johnston, R. C. Doty, B. A. Korgel, *Science* **2000**, *287*, 1471.
[50] T. Hanrath, B. A. Korgel, *Adv. Mater.* **2003**, *15*, 437–440.
[51] A. Dorn, C. R. Wong, M. G. Bawendi, *Adv. Mater.* **2009**, *21*, 3479–3482.
[52] A. Dorn, P. M. Allen, M. G. Bawendi, *ACS Nano* **2009**, *3*, 3260–3265.
[53] H. Yu, W. E. Buhro, *Adv. Mater.* **2003**, *15*, 416–419.
[54] H. Yu, P. C. Gibbons, K. F. Kelton, W. E. Buhro, *J. Am. Chem. Soc.* **2001**, *123*, 9198–9199.
[55] H. Yu, J. Li, R. A. Loomis, L. W. Wang, W. E. Buhro, *Nat. Mater.* **2003**, *2*, 517–520.
[56] D. D. Fanfair, B. A. Korgel, *Cryst. Growth Des.* **2005**, *5*, 1971–1976.
[57] T. J. Trentler, S. C. Goel, K. M. Hickman, A. M. Viano, M. Y. Chiang, A. M. Beatty, P. C. Gibbons, W. E. Buhro, *J. Am. Chem. Soc.* **1997**, *119*, 2172–2181.
[58] S. Kan, A. Aharoni, T. Mokari, U. Banin, *J. Chem. Soc. Faraday Trans.* **2004**, *125*, 23–38.

[59] A. Dong, H. Yu, F. Wang, W. E. Buhro, *J. Am. Chem. Soc.* **2008**, *130*, 5954–5961.
[60] H. Yu, J. Li, R. A. Loomis, P. C. Gibbons, L. W. Wang, W. E. Buhro, *J. Am. Chem. Soc.* **2003**, *125*, 16168–16169.
[61] J. W. Grebinski, K. L. Hull, J. Zhang, T. H. Kosel, M. Kuno, *Chem. Mater.* **2004**, *16*, 5260–5272.
[62] L. Ouyang, K. N. Maher, C. L. Yu, J. McCarty, H. Park, *J. Am. Chem. Soc.* **2007**, *129*, 133–138.
[63] A. Dong, F. Wang, T. L. Daulton, W. E. Buhro, *Nano Lett.* **2007**, *7*, 1308–1313.
[64] D. D. Fanfair, B. A. Korgel, *Cryst. Growth Des.* **2008**, *8*, 3246–3252.
[65] Z. Li, O. Kurtulus, N. Fu, Z. Wang, A. Kornowski, U. Pietsch, A. Mews, *Adv. Funct. Mater.* **2009**, *19*, 3650–3661.
[66] A. Huczko, *Appl. Phys. A: Mater. Sci. Process.* **2000**, *70*, 365–376.
[67] J. C. Hulteen, C. R. Martin, *J. Mater. Chem.* **1997**, *7*, 1075–1087.
[68] Y. Xia, P. Yang, Y. Sun, Y. Wu, B. Mayers, B. Gates, Y. Yin, F. Kim, H. Yan, *Adv. Mater.* **2003**, *15*, 353–389.
[69] C. Brinker, Y. Lu, A. Sellinger, H. Fan, *Adv. Mater.* **1999**, *11*, 579–585.
[70] C. N. R. Rao, A. Govindaraj, F. L. Deepak, N. A. Gunari, M. Nath, *Appl. Phys. Lett.* **2001**, *78*, 1853.
[71] R. Lv, C. Cao, H. Zhai, D. Wang, S. Liu, H. Zhu, *Solid State Commun.* **2004**, *130*, 241–245.
[72] Y. Liu, J. Cao, J. Zeng, C. Li, Y. Qian, S. Zhang, *Eur. J. Inorg. Chem.* **2003**, 644–647.
[73] Y. Yin, Y. Lu, Y. Sun, Y. Xia, *Nano Lett.* **2002**, *2*, 427–430.
[74] B. Gates, Y. Wu, Y. Yin, P. Yang, Y. Xia, *J. Am. Chem. Soc.* **2001**, *123*, 11500–11501.
[75] B. Gates, B. Mayers, Y. Wu, Y. Sun, B. Cattle, P. Yang, Y. Xia, *Adv. Funct. Mater.* **2002**, *12*, 679–686.
[76] Z. Y. Jiang, Z. X. Xie, X. H. Zhang, R. B. Huang, L. S. Zheng, *Chem. Phys. Lett.* **2003**, *378*, 313–316.
[77] U. Jeong, Y. Xia, Y. Yin, *Chem. Phys. Lett.* **2005**, *416*, 246–250.
[78] W. I. Park, H. S. Kim, S. Y. Jang, J. Park, S. Y. Bae, M. Jung, H. Lee, J. Kim, *J. Mater. Chem.* **2008**, *18*, 875–880.
[79] G. D. Moon, S. Ko, Y. Xia, U. Jeong, *ACS Nano* **2010**, *4*, 2307–2319.
[80] M. Lai, D. J. Riley, *J. Colloid Interf. Sci.* **2008**, *323*, 203–212.
[81] D. Lincot, *Thin Solid Films* **2005**, *487*, 40–48.
[82] D. Routkevitch, T. Bigioni, M. Moskovits, J. M. Xu, *J. Phys. Chem.* **1996**, *100*, 14037–14047.
[83] D. J. Pena, J. K. N. Mbindyo, A. J. Carado, T. E. Mallouk, C. D. Keating, B. Razavi, T. S. Mayer, *J. Phys. Chem. B* **2002**, *106*, 7458–7462.
[84] M. J. Zheng, L. D. Zhang, G. H. Li, W. Z. Shen, *Chem. Phys. Lett.* **2002**, *363*, 123–128.
[85] L. Li, Y. Yang, X. Huang, G. Li, L. Zhang, *J. Phys. Chem. B* **2005**, *109*, 12394–12398.
[86] J. Mallet, M. Molinari, F. Martineau, F. Delavoie, P. Fricoteaux, M. Troyon, *Nano Lett.* **2008**, *8*, 3468–3474.
[87] I. Lombardi, A. I. Hochbaum, P. Yang, C. Carraro, R. Maboudian, *Chem. Mater.* **2006**, *18*, 988–991.
[88] T. Shimizu, T. Xie, J. Nishikawa, S. Shingubara, S. Senz, U. Gosele, *Adv. Mater.* **2007**, *19*, 917–920.
[89] Z. A. Peng, X. Peng, *J. Am. Chem. Soc.* **2002**, *124*, 3343–3353.
[90] B. Sun, E. Marx, N. C. Greenham, *Nano Lett.* **2003**, *3*, 961–963.
[91] W. U. Huynh, J. J. Dittmer, A. P. Alivisatos, *Science* **2002**, *295*, 2425.
[92] I. Gur, N. A. Fromer, M. L. Geier, A. P. Alivisatos, *Science* **2005**, *310*, 462.
[93] M. Law, L. E. Greene, J. C. Johnson, R. Saykally, P. Yang, *Nat. Mater.* **2005**, *4*, 455–459.
[94] L. E. Green, M. Law, J. Goldberger, F. Kim, J. C. Johnson, Y. Zhang, R. J. Saykally, P. Yang, *Angew. Chem. Int. Ed.* **2003**, *42*, 3031–3034.
[95] S. H. Kang, S. H. Choi, M. S. Kang, J. Y. Kim, H. S. Kim, T. Hyeon, Y. E. Sung, *Adv. Mater.* **2008**, *20*, 54–58.
[96] K. S. Leschkies, R. Divakar, J. Basu, E. Enache-Pommer, J. E. Boercker, C. B. Carter, U. R. Kortshagen, D. J. Norris, E. S. Aydil, *Nano Lett.* **2007**, *7*, 1793–1798.
[97] R. Vogel, K. Pohl, H. Weller, *Chem. Phys. Lett.* **1990**, *174*, 241–246.
[98] R. Vogel, P. Hoyer, H. Weller, *J. Phys. Chem.* **1994**, *98*, 3183–3188.

Received: July 3, 2010
Published Online: August 27, 2010

